

**Assessment of Vulnerable Plaques Causing Acute Coronary Syndrome Using
Integrated Backscatter Intravascular Ultrasound**

Keiji Sano, Masanori Kawasaki, Yoshiyuki Ishihara, Munenori Okubo, Kunihiko
Tsuchiya, Kazuhiko Nishigaki, Xiangrong Zhou, Shinya Minatoguchi, Hiroshi
Fujita, and Hisayoshi Fujiwara

J. Am. Coll. Cardiol. published online Feb 6, 2006;

doi:10.1016/j.jacc.2005.09.061

This information is current as of February 10, 2012

The online version of this article, along with updated information and services, is
located on the World Wide Web at:

<http://content.onlinejacc.org/cgi/content/full/j.jacc.2005.09.061v1>

JACC

JOURNAL of the AMERICAN COLLEGE of CARDIOLOGY



Assessment of Vulnerable Plaques Causing Acute Coronary Syndrome Using Integrated Backscatter Intravascular Ultrasound

Keiji Sano, MD, PhD,* Masanori Kawasaki, MD, PhD,* Yoshiyuki Ishihara, MD,* Munenori Okubo, MD,* Kunihiro Tsuchiya, MD, PhD,* Kazuhiko Nishigaki, MD, PhD,* Xiangrong Zhou, PhD,† Shinya Minatoguchi, MD, PhD,* Hiroshi Fujita, PhD,† Hisayoshi Fujiwara, MD, PhD*

Gifu, Japan

OBJECTIVES	This study aims to define tissue characteristics of vulnerable plaques before acute coronary syndrome (ACS) by use of integrated backscatter intravascular ultrasound (IB-IVUS).
BACKGROUND	Tissue characterization of coronary plaques is possible with the use of IB-IVUS.
METHODS	The subjects were 140 patients with angina pectoris, and we selected 160 coronary lesions without significant stenosis for evaluation. Ultrasound signals were obtained by an IVUS system using a 40-MHz catheter.
RESULTS	At the follow-up (30 ± 7 months), 12 plaques caused ACS after the initial IVUS examination. Ten of the 12 plaques had IVUS parameters recorded at baseline. These 10 plaques were classified as vulnerable plaques (VP), and the other plaques were classified as stable plaques (SP; $n = 143$). There was no significant difference of vessel area, lumen area, and plaque area between VP and SP. However, plaque burden ($60 \pm 9\%$ vs. $52 \pm 9\%$; $p = 0.014$), eccentricity (0.70 ± 0.10 vs. 0.55 ± 0.17 ; $p = 0.013$), remodeling index (1.30 ± 0.08 vs. 1.16 ± 0.16 ; $p = 0.006$) and percentage lipid area ($72 \pm 10\%$ vs. $50 \pm 16\%$; $p < 0.0001$) were greater in VP than in SP. Percentage fibrous area ($23 \pm 6\%$ vs. $47 \pm 14\%$; $p < 0.0001$) was smaller in VP than in SP. The sensitivities, specificities, and positive predictive values of percentage fibrous area (90%, 96%, and 69%, respectively) and percentage lipid area (80%, 90%, and 42%, respectively) for classifying VP were evaluated.
CONCLUSIONS	Tissue characteristics of VP before ACS were different from those of SP. This suggests that VP and SP as classified by IB-IVUS are useful in predicting ACS. (J Am Coll Cardiol 2006;47:734–41) © 2006 by the American College of Cardiology Foundation

Pathologic and angiographic studies have demonstrated that disruption or erosion of vulnerable plaques and subsequent thromboses are the most frequent cause of acute coronary syndromes (ACS) (1,2). Postmortem studies have identified several histologic characteristics of these vulnerable plaques, such as a high-lipid core area and a thin fibrous cap (3,4). Previous angiographic studies reported that pre-existing coronary stenosis in patients with first myocardial infarction is not necessarily severe. The culprit coronary lesion in the patients with unstable angina showed a relatively minor stenosis, <50% of the luminal diameter (5,6).

Intravascular ultrasound (IVUS) allows cross-sectional imaging of coronary arteries and provides a more comprehensive assessment of the atherosclerotic plaques in vivo. Studies using IVUS have indicated that the coronary atherosclerosis is underestimated when visually analyzing angiography results owing to the coronary compensatory remodeling and the diffuse nature of coronary atherosclerosis, which frequently makes the reference vessel appear normal angiographically (7). To date, IVUS has contributed to our understanding of the progression and regression of

coronary plaque. Glagov et al. (8) demonstrated that compensatory enlargement of the vessel prevents the atheroma from encroaching on the lumen, thereby concealing the presence of a lesion when using angiography. However, there are no precise data about tissue components of vulnerable plaque in vivo, because there is no way of analyzing the components clinically. It may be difficult to predict the site of a subsequent occlusion from a conventional IVUS study, because it is difficult to quantitatively differentiate lipid component from fibrous tissue using conventional IVUS.

Recently, we have developed an integrated backscatter intravascular ultrasound (IB-IVUS) system in which two-dimensional (2D) color-coded maps of plaque tissue characterization in coronary arteries were constructed by computer (9). The purpose of the present study is to define the tissue characteristics of vulnerable plaques before ACS using IB-IVUS and to elucidate the feasibility of certain parameters for the prediction of ACS in clinical settings.

METHODS

Patients and study design. This study was a follow-up of nontarget coronary lesions with moderate stenosis (diameter stenosis 25% to 50%) in patients with stable angina pectoris who underwent percutaneous coronary intervention (PCI). Patients were consecutively enrolled from September 2001

From the *Division of Regeneration and Advanced Medical Science and the †Department of Intelligent Image Information, Gifu University Graduate School of Medicine, Gifu, Japan. This study was supported, in part, by a research grants 15590731 (2003) and Frontier Medicine (2002–2004) from the Ministry of Education, Culture, Sports, Science and Technology of Japan.

Manuscript received June 6, 2005; revised manuscript received September 16, 2005, accepted September 19, 2005.

Abbreviations and Acronyms

ACS	= acute coronary syndrome
CSA	= cross-sectional area
EEM	= external elastic membrane
IB	= integrated backscatter
IVUS	= intravascular ultrasound
LCSA	= lumen cross-sectional area
PCI	= percutaneous coronary intervention
ROI	= region of interest
SP	= stable plaques
VP	= vulnerable plaques

to June 2003. The institutional ethics committee approved the protocol, and informed consent was obtained from all patients and their relatives. Patients were excluded if they had unstable angina or myocardial infarction within the previous three months, an ejection fraction of $\leq 30\%$, total serum cholesterol >240 mg/dl with or without statin therapy, or severe hypertriglyceridemia (>400 mg/dl). A total of 140 patients with stable angina pectoris were enrolled in the study. Integrated backscatter IVUS was performed in each patient in one or two arterial segments without significant stenosis. The nontargeted plaques analyzed had to be more than 20 mm from the target site. Another coronary artery was analyzed if there was no plaque with moderate stenosis in the vessel with the target lesion. In the follow-up period, the diagnosis of acute myocardial infarction was based on elevation at least one positive biomarker (creatinine kinase [CK], CK-MB, CK-MB mass (CK-MBm), or troponin), and at least two measurements of the same maker were obtained at least 6 h apart. In addition, the diagnosis required characteristic electrocardiogram changes and a history of prolonged acute chest, epigastric, neck, jaw, or arm pain. Unstable angina was defined as either angina with a progressive crescendo pattern or angina that occurred at rest. Coronary angiography was performed within 24 h after the onset of ACS and within 12 h after the patients arrived at our hospital.

IB system presets and data acquisition. Conventional IVUS images and ultrasound signals were acquired during the diastolic phase using a commercially available IVUS imaging system (Clear View; Boston Scientific, Natick, Massachusetts) and an analog-digital converter (Wavepro 960; LeCroy, Chestnut Ridge, New York) to characterize the coronary arterial tissue using a 40-MHz intravascular catheter. During routine PCI, we administered an intracoronary optimal dose of isosorbide dinitrate before the measurements for the prevention of coronary spasm. A total of 18 IB-IVUS images were captured at an interval of 1 mm using a motorized pull-back system in each plaque. Then the segment with the minimum lumen area was evaluated in each plaque. We used 256 vector lines per image (1.4 grade/line) and set 20 regions of interest (ROIs) for each 100- μ m depth on each vector line (total 5,120 ROIs/image). Integrated backscatter values were calculated as

previously described (9). To make the quantitative area analysis more accurate, polar coordinates were transformed into Cartesian coordinates (64×64 pixels), using a computer algorithm previously described, because the size of each ROI in the polar coordinates was different (10). We then manually selected the intima in the color-coded maps for calculation of the number of pixels. Our definition of IB values for each histologic category was determined by comparing histologic images, as reported in our previous study (9).

Conventional IVUS and IB-IVUS parameters. Each conventional IVUS and IB-IVUS parameter at baseline was measured in the plaques and subjected to statistical analysis. The IVUS measurements were performed by two experienced IVUS readers. In the conventional IVUS analysis, cross-sectional images were quantified for lumen cross-sectional area (LCSA), external elastic membrane (EEM) cross-sectional area (CSA), and plaque (P) + media (M) cross-sectional area (P+M CSA = EEM CSA – LCSA) using the software included with the IVUS system. In the present study, the interobserver correlation coefficient was 0.98 for EEM, 0.97 for LCSA, and 0.97 for P+M CSA. The P+M eccentricity rate was calculated as (maximum P+M thickness – minimum P+M thickness)/maximum P+M thickness. The remodeling index was defined as the ratio of EEM CSA at the measured lesion (minimum luminal site) to reference EEM CSA (the average of the proximal and distal reference segments). After the color-coded maps were transformed into Cartesian coordinates, the percentage fibrous area (fibrous area/plaque area) and the percentage lipid area (lipid area/plaque area) were automatically counted by use of commercially available computer software (T3D, Fortner Research, Sterling, Virginia). The validation has been reported previously: The intraobserver and interobserver variability of the area of lipid pool were $4.2 \pm 2.8\%$ and $5.3 \pm 3.3\%$, respectively. The intraobserver and interobserver correlation of the area of lipid pool was $r = 0.91$ ($p < 0.01$) and $r = 0.90$ ($p < 0.01$), respectively (11).

Statistical analyses. Laboratory and ultrasound parameters were reported as the mean \pm SD. An unpaired Student *t* test was used to compare the parameters between vulnerable plaques (VP) and stable plaque (SP). Receiver operating characteristic (ROC) curves were used to determine the cutoffs of IVUS parameters as a marker for classification of VP. For estimation of diagnostic accuracies, the sensitivities, specificities, positive predictive values, negative predictive values, and accuracies of the IVUS parameters were calculated at the cutoffs determined by the ROC curves. A *p* value of <0.05 was considered statistically significant.

RESULTS

Characteristics of the patient with and without ACS. One hundred sixty angina-unrelated coronary lesions in 160 coronary arteries without significant stenosis were evaluated

in this study. At the follow-up (mean 30 ± 7 months), 12 plaques caused ACS at an average of 7.6 ± 6.1 months after the initial IVUS examination. Ten of the 12 plaques had IVUS parameters recorded. Two plaques in two patients, who suffered ACS but whose culprit lesions had not been investigated, were excluded from the study. In the five patients who had ACS at one site, the remaining imaged site was excluded from comparison, because the behavior of various plaques within the same patient are not likely to be independent. Finally, 153 plaques were classified as either VP ($n = 10$) that caused ACS or SP ($n = 143$) that did not cause ACS. There was no significant difference in characteristics, blood lipid levels, or the rate of concomitant medications at baseline between the patients with ACS and without ACS (Table 1).

Quantitative parameters of conventional IVUS and IB-IVUS. Table 2 shows quantitative IVUS findings. There was no significant difference in the percentage diameter stenosis between VP ($35 \pm 7\%$) and SP ($31 \pm 7\%$). Also, there was no significant difference in EEM-CSA, LCSA, and P+M CSA between VP and SP. However, plaque burden ($60 \pm 9\%$ vs. $52 \pm 9\%$; $p = 0.014$), eccentricity rate

Table 1. Baseline Clinical and Laboratory Characteristics of Patients With or Without ACS

	Patients With ACS (n = 10)	Patients Without ACS (n = 128)	p
Gender			
Men	6 (60)	87 (68)	0.60
Age, yrs	67 ± 8	68 ± 9	0.89
Clinical history			
Myocardial infarction	1 (10)	18 (14)	0.71
Previous coronary bypass graft	0 (0)	3 (2)	0.62
Hypertension	6 (60)	80 (63)	0.87
Hyperlipidemia	5 (50)	63 (49)	0.96
Current smoker	2 (20)	21 (16)	0.78
Diabetes mellitus type 2	3 (30)	25 (19)	0.42
Coronary artery disease			
Multiple vessel	5 (50)	53 (65)	0.89
Target plaque location			
LAD	5 (50)	60 (47)	0.85
LCX	2 (20)	35 (27)	0.61
RCA	3 (30)	33 (23)	0.77
Medication			
Aspirin	10 (100)	128 (100)	1.0
Ticlopidine	10 (100)	128 (100)	1.0
Statin	4 (40)	48 (38)	0.87
Nirates	6 (60)	68 (53)	0.67
Calcium-channel blockers	5 (50)	78 (61)	0.50
Beta-blockers	2 (20)	28 (22)	0.89
Insulin	3 (30)	16 (13)	0.12
ACE inhibitors	4 (40)	55 (43)	0.86
Blood lipid levels (mg/dl)			
Total cholesterol	212 ± 48	201 ± 34	0.31
Triglycerides	136 ± 79	137 ± 67	0.94
HDL cholesterol	43 ± 5	49 ± 12	0.11
LDL cholesterol	134 ± 34	125 ± 29	0.15

Values are n (%) or mean \pm SD.

ACE = angiotensin-converting enzyme; ACS = acute coronary syndromes; HDL = high-density lipoprotein; LAD = left anterior descending coronary artery; LCX = left circumflex artery; LDL = low-density lipoprotein; RCA = right coronary artery.

Table 2. Baseline Intravascular Ultrasound Characteristics

	Vulnerable Plaques (n = 10)	Stable Plaques (n = 143)	p
Vessel area, mm ²	13.9 ± 2.0	14.2 ± 3.5	0.72
Lumen area, mm ²	6.1 ± 1.2	6.7 ± 2.0	0.31
Plaque area, mm ²	8.0 ± 2.0	7.5 ± 2.4	0.41
Plaque burden, %	60 ± 9	52 ± 9	0.014
Diameter stenosis, %	35 ± 7	31 ± 7	0.10
Area stenosis, %	57 ± 8	52 ± 9	0.09
Eccentricity rate	0.70 ± 0.10	0.55 ± 0.17	0.013
Remodeling index	1.30 ± 0.08	1.16 ± 0.16	0.006
Fibrous area, %	23 ± 6	47 ± 14	<0.0001
Lipid area, %	72 ± 10	50 ± 16	<0.0001

Values are mean \pm SD.

(0.70 ± 0.10 vs. 0.55 ± 0.17 ; $p = 0.013$), remodeling index (1.30 ± 0.08 vs. 1.16 ± 0.16 ; $p = 0.006$), and the percentage lipid area ($72 \pm 10\%$ vs. $50 \pm 16\%$; $p < 0.0001$) of VP were greater than those of SP. Furthermore, the percentage fibrous area was smaller in VP ($23 \pm 6\%$) than in SP ($47 \pm 14\%$) ($p < 0.0001$).

Parameters of conventional IVUS and IB-IVUS for predicting ACS. Representative VP and SP are shown in Figures 1 to 3. These figures indicate that VP had greater lipid area and smaller fibrous area than SP. The optimal cutoffs for the calculation of diagnostic accuracy to classify VP were obtained from the ROC curve (Fig. 4). The optimal cutoffs of percentage fibrous area, percentage lipid area, remodeling index, eccentricity rate, and plaque burden were 25%, 65%, 1.25, 0.65, and 55%, respectively. The percentage fibrous area was the most sensitive of all IVUS parameters for classifying VP (area under curve = 0.98). Among 10 VP, 9 (90%) had a fibrous area of $\leq 25\%$, whereas only 6 (4%) SP had a fibrous area of $\leq 25\%$. Sensitivities, specificities, positive predicting values, negative predictive values, and accuracies for each parameter at the optimal cutoffs values are shown in Table 3. Multivariate logistic regression analysis did not detect independent predictors of ACS.

DISCUSSION

Recently, many techniques for the tissue characterization of plaque composition have been developed using mathematical analyses of ultrasound signals (12–15). We developed an IB-IVUS system for tissue characterization of coronary plaques using fast Fourier transform (9). The present equipment with an IVUS system and a commercially available digital analog converter made qualitative analysis of images possible without any reconstruction of video recorder images.

Frequency of occurrence of ACS. According to previous findings, progression of coronary artery disease is seen in 7% to 12% of lesions per year (16–18). In a recent study, the rate of occurrence of ACS during a follow-up period of 21.8 ± 6.4 months was 7.5% per year (19). In the present study, the rate of occurrence of ACS in the follow-up

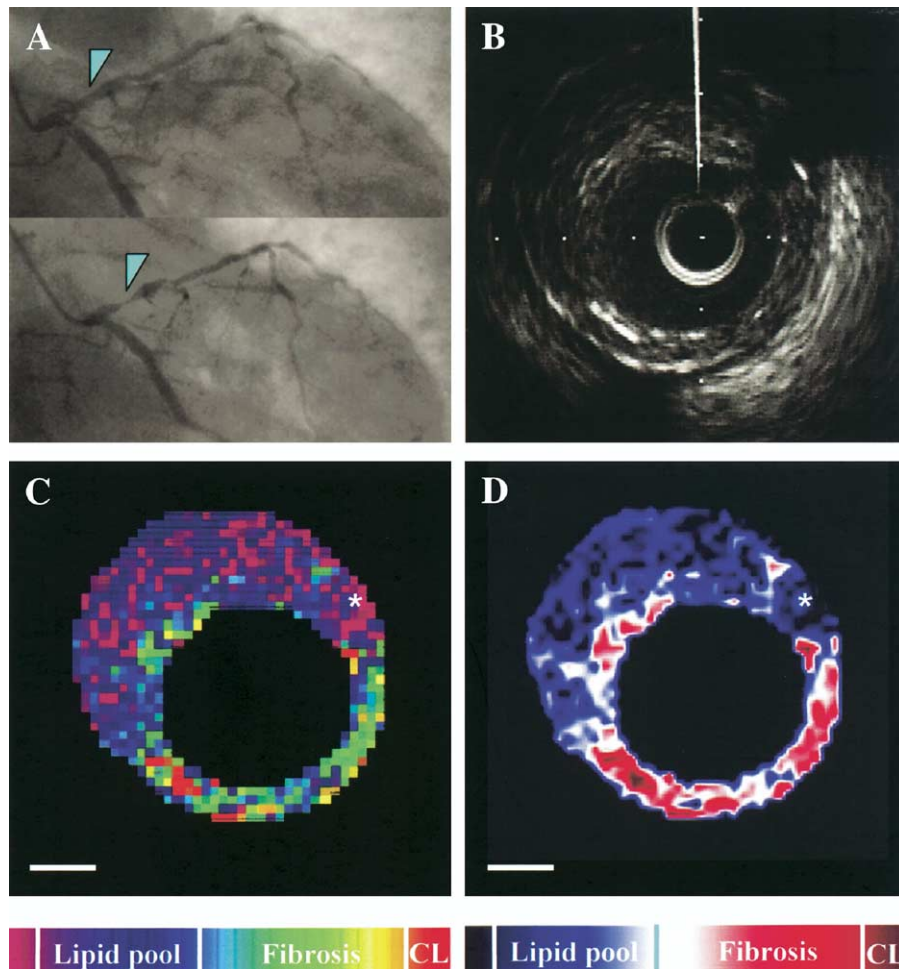


Figure 1. Images of the culprit lesion causing acute coronary syndrome. (A) Angiography of the left coronary artery. (Upper) The arrowhead indicates a lesion, in which intravascular ultrasound (IVUS) measurements were recorded at baseline. (Lower) The arrowhead indicates the culprit lesion at follow-up. (B) Conventional IVUS image of segment indicated by the arrowhead in A. (C) Integrated backscatter (IB)-IVUS image of Cartesian coordinates, constructed using conventional color gradation, of the segment indicated by the arrowhead in A. The asterisk indicates the guidewire artifact. Note the large lipid core (blue) with fibrous cap (green). (D) IB-IVUS image of Cartesian coordinates, constructed using another color gradation, of the segment indicated by the arrowhead in A. This type of color-coded map illustrates the difference between lipid pool and fibrous tissue. The asterisk indicates the guidewire artifact. Note the large lipid core (blue) with fibrous cap (red or white). CL = calcification. Bar = 1 mm.

period of 30 ± 7 months was 3.4% per year (12 of 140 patients/2.5 years). Although different criteria were used to define disease progression, the rate of disease progression in the present study was less than the previous reports. Furthermore, the lower rate of disease progression in the present study may have been due to the frequent use of HMG-Co-A reductase inhibitors (statins), because there is ample evidence that statins reduce the progression of atherosclerosis (20,21). Actually, a recent study showed that 5.8% of coronary lesions required additional PCI of non-target lesions because of plaque progression at one year and that the majority (86.9%) of these lesions were $\leq 60\%$ in severity (mean stenosis 41.8%) at the time of the initial PCI (22). The progression and stenosis rate in the present study was similar to that in this previous study. Although the average follow-up period was 30 months, it is surprising that ACS developed an average of only 7.6 months after IVUS imaging. This result is similar to the time required for the

development of ACS (4.0 ± 3.4 months, range 1 to 8 months) in a previous report (19). The relatively early development of ACS after IVUS imaging is likely to increase the predictive values of IVUS for classifying vulnerable plaques, and the predictive values are likely to be lower at a later time point. Although the reason for the early development of ACS is unknown, the subjects in the present study were patients with angina pectoris that underwent PCI. Such a rapid development of ACS probably involves diffuse destabilization of coronary plaques, leading to the condition of “pancoronary,” as suggested in recent IVUS and angiographic studies (23,24).

Conventional IVUS and IB-IVUS parameters. There are several reports showing the details of the plaques that caused ACS by use of conventional IVUS. It was reported that 30% of ruptured plaques contained hypoechoic, 31% hyperechoic, and 39% mixed plaque. The site of the original tear in

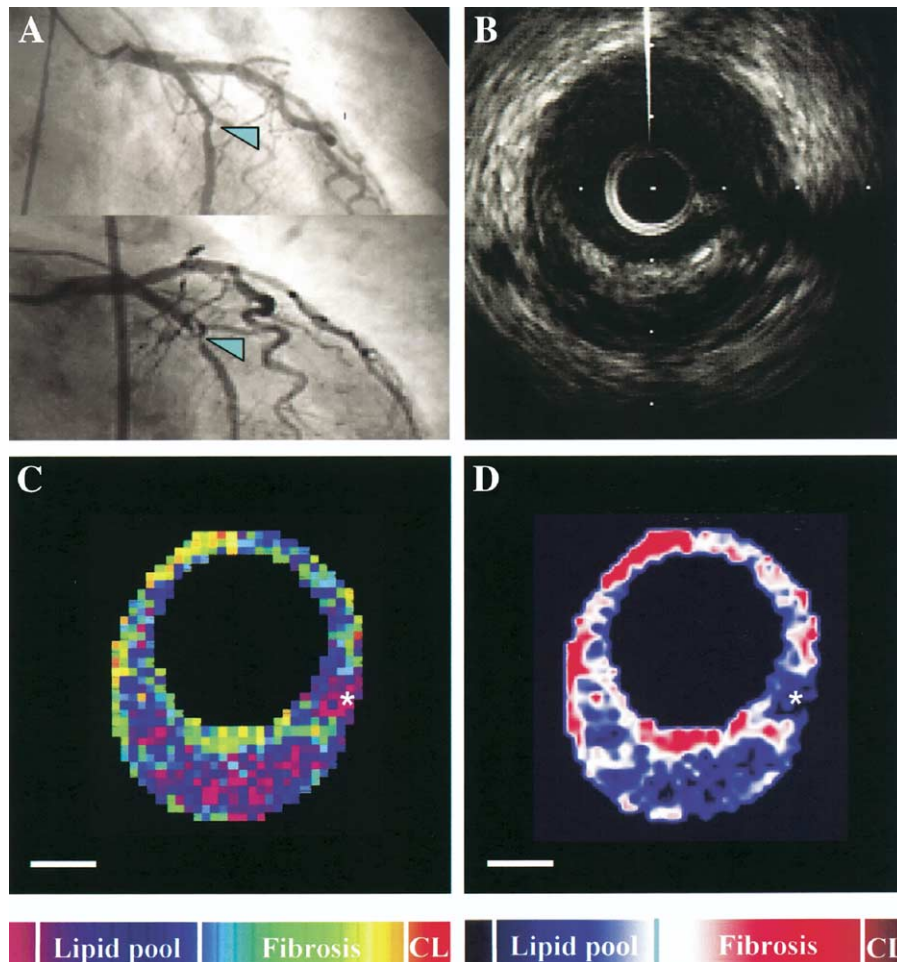


Figure 2. Images of the culprit lesion causing acute coronary syndrome. (A) Angiography of the circumflex coronary artery. (Upper) The arrowhead indicates a lesion, in which IVUS measurements were recorded at baseline. (Lower) The arrowhead indicates the culprit lesion at follow-up. (B) Conventional intravascular ultrasound (IVUS) image of the segment indicated by the arrowhead in A. (C) Integrated backscatter (IB)-IVUS image of Cartesian coordinates, constructed using conventional color gradation, of the segment indicated by the arrowhead in A. The asterisk indicates the guidewire artifact. Note the large lipid core (blue) with fibrous cap (green). (D) IB-IVUS image of Cartesian coordinates, constructed using another color gradation, of the segment indicated by the arrowhead in A. The asterisk indicates the guidewire artifact. Note the large lipid core (blue) with fibrous cap (red or white). CL = calcification. Bar = 1 mm.

the fibrous cap could be identified; 63% of tears appeared to have occurred at the shoulder of the plaque and the remaining 37% in the center of the plaque (25). According to another report, 70% of patients with ACS had at least one atherosclerotic lesion that had rupture criteria in an artery distinct from the culprit artery (23). Fujii et al. (26) reported that ruptured plaques in culprit lesions of ACS patients had smaller lumens, greater plaque burdens, area stenosis, and remodeling indices, and more thrombus. Although these reports provided important insight into plaques ruptured in ACS, they were studies focusing on plaques after the occurrence of rupture.

There are few data using IVUS to define the feature of VP before the occurrence of ACS. Yamagishi et al. (19) has shown the morphology of VP before ACS. In that study, 16 of 106 patients had acute coronary events during a follow-up period of 21.8 ± 6.4 months. The pre-existing plaques before ACS had shallow echolucent zones with compensatory plaque

enlargement. Regarding conventional IVUS parameters, this study showed that the plaque burden of the plaques leading to ACS exhibited an eccentric pattern that was greater than those in the patients without ACS. Another study demonstrated that the lesion eccentricity index and the remodeling ratio of plaques that caused ACS were greater than those of plaques that were associated with stable angina (27). Moreover, studies examining the differences between ruptured plaques and nonruptured plaques in the same coronary artery demonstrated that the lumen eccentricity index of ruptured plaques was greater than that of nonruptured plaques (28). Regarding IB-IVUS parameters, percentage lipid areas were greater in VP than in SP. Moreover, percentage fibrous areas were smaller in SP than in VP. Previous pathologic studies of VP after ACS have demonstrated that large lipid cores are recognized histologic markers for plaque vulnerability (29). Our findings are in agreement with these previous results.

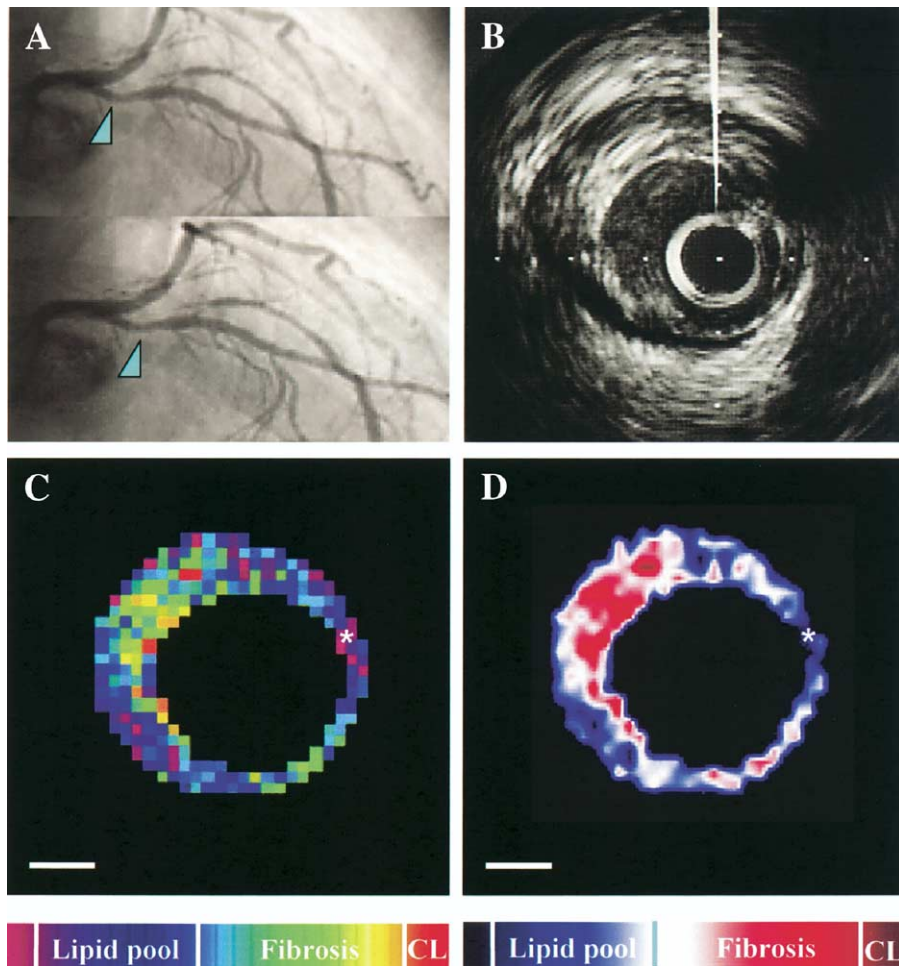


Figure 3. Images of the lesion not causing acute coronary syndrome. (A) Angiography of the left coronary artery. (Upper) The arrowhead indicates a lesion, in which intravascular ultrasound (IVUS) measurements were recorded at baseline. (Lower) the arrowhead indicates the segment indicated by the arrowhead at baseline after the follow-up period. (B) Conventional IVUS image of the segment indicated by the arrowhead in A. (C) Integrated backscatter (IB)-IVUS image of Cartesian coordinates, constructed using conventional color gradation, of the segment indicated by the arrowhead in A. The asterisk indicates the guidewire artifact. Note the small lipid core (blue) with large fibrous tissue (green). (D) IB-IVUS image of Cartesian coordinates, constructed using another color gradation, of the segment indicated by the arrowhead in A. The asterisk indicates the guidewire artifact. Note the small lipid core (blue) with large fibrous tissue (red or white). CL = calcification. Bar = 1 mm.

Diagnostic values of IB-IVUS to classify VP. In the IVUS parameters in which there were significant differences between SP and VP in the present study, the optimal cutoffs for classifying VP were determined by use of ROC curves. The AUC showed that percentage fibrous area was the most useful parameter to classify VP. To determine cutoffs for classifying VP, there is the restriction that plaques may have caused ACS after the follow-up period. Therefore, we probably underestimated the number of VP because we could not identify the plaques causing ACS after the follow-up period. Using percentage lipid area of $>65\%$ as a cutoff, IB-IVUS was positive in 8 plaques and negative in 11 plaques. This resulted in a low positive predictive value of 42% for predicting ACS. Similar low positive predictive values for classifying VP were obtained using plaque burden, remodeling index, and eccentricity rate. Therefore, we also employed second cutoffs for each parameter to increase the positive predictive value rather than to maintain a high

sensitivity. However, the positive predictive value of each parameter at the second cutoff did not increase, as shown in Table 3.

Plaque rupture is related to the process in which fibrous caps over lipid core become fragile. Prior studies reported that shear stress and circumferential wall stress play an important role in plaque rupture (30). To differentiate VP from SP, the fragile part of the atheromatous plaque is of major interest. For the purpose of detecting fragile parts of plaques, IVUS elastography has been validated to distinguish different plaque features in vivo (14). For the prediction of ACS, both tissue characteristics of coronary plaques and the mechanical stresses on coronary plaques should be taken into account.

Study limitations. First, the subjects of the present study were the patients with angina pectoris that required PCI. In addition, some selection bias was inevitable because we selected one or two plaques in each patient. Therefore,

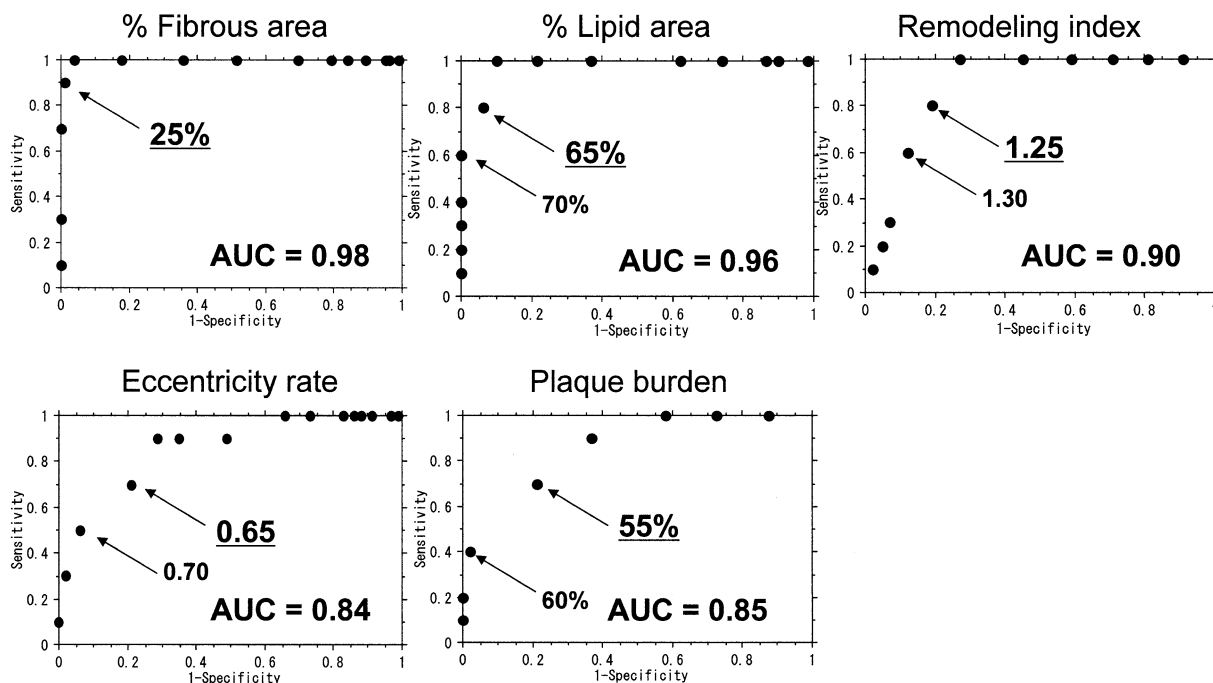


Figure 4. Receiver operating characteristic curves for each intravascular ultrasound parameter. Optimal cutoffs are indicated by underlining. Secondary selected cutoffs were indicated without underline. Note that area under curves (AUCs) show that percentage fibrous area was the most sensitive parameter for classifying the plaques causing acute coronary syndrome.

the findings of the present study may not be applicable to the general population. Second, there was a possibility that the components and morphologies of plaques may have changed during the follow-up period between the initial IVUS examination and the development of ACS. Plaques could change in size, morphology, or tissue characteristics. Serial IVUS observations would be required to demonstrate changes in plaques, although we did not believe it is appropriate to perform serial IVUS because it is an invasive method. Third, calcification is a perfect reflector for ultrasound, causing the acoustic

shadowing typically observed in IVUS images. In addition, we excluded the area of the artifact due to the guidewire from the IB-IVUS analyses. Therefore, the guidewire artifact and calcification hinder a rigorous calculation of the area of each component. Finally, because the number of plaques causing ACS was small, multivariate logistic regression analysis did not detect independent predictors of ACS, and the statistical power of the ROC curve analysis for the predicting ACS was low, particularly when the area under the ROC curve was 0.98. Furthermore, plaques defined as SP might cause

Table 3. Assessment of IB-IVUS and Conventional IVUS Parameters for Classifying Vulnerable Plaques

	Sensitivity	Specificity	PPV	NPV	Accuracy
Optimal cutoffs					
IB-IVUS					
% Fibrous area (cutoff <25%)	90 (85–95)	96 (93–99)	69 (62–76)	99 (97–100)	95 (92–98)
% Lipid area (cutoff >65%)	80 (74–86)	90 (85–95)	42 (34–50)	98 (96–100)	89 (84–94)
Conventional IVUS					
Plaque burden (cutoff >55%)	70 (63–77)	63 (55–69)	17 (11–23)	95 (92–98)	63 (55–69)
Remodeling index (cutoff >1.25)	80 (74–86)	81 (75–87)	30 (23–37)	97 (94–100)	81 (75–87)
Eccentricity rate (cutoff >0.65)	70 (63–77)	69 (62–76)	18 (12–24)	96 (93–99)	69 (62–76)
Secondary selected cutoffs					
IB-IVUS					
% Lipid area (cutoff >70%)	60 (52–68)	93 (89–97)	46 (38–54)	96 (93–99)	91 (86–96)
Conventional IVUS					
Plaque burden (cutoff >60%)	40 (32–48)	79 (73–85)	17 (11–23)	93 (89–97)	75 (68–82)
Remodeling index (cutoff >1.30)	30 (23–37)	88 (83–93)	20 (14–26)	92 (88–96)	86 (81–91)
Eccentricity rate (cutoff >0.70)	50 (42–58)	79 (73–85)	20 (14–26)	94 (90–98)	76 (69–83)

Data are percentages (95% confidence intervals).

IB = integrated backscatter; IVUS = intravascular ultrasound; NPV = negative predictive value; PPV = positive predictive value.

ACS after the follow-up period, which would lower the positive predictive value. Large-scale long-term studies are required to address this limitation.

Conclusions. We reported in detail the prognostic utility of morphologic and tissue characteristics of VP before ACS. Tissue characteristics of VP before ACS were different from those of SP. This suggests that VP and SP as classified by IB-IVUS are useful in predicting ACS.

Reprint requests and correspondence: Dr. Hisayoshi Fujiwara, Regeneration and Advanced Medical Science, Gifu University Graduate School of Medicine, Gifu, Japan, 1-1 Yanagido, Gifu 501-1194, Japan. E-mail: gifuim-gif@umin.ac.jp.

REFERENCES

- Mizuno K, Satomura K, Miyamoto A, et al. Angioscopic evaluation of coronary artery thrombi in acute coronary syndromes. *N Engl J Med* 1992;326:287–91.
- Fuster V, Badimon L, Badimon JJ, et al. The pathogenesis of coronary artery disease and the acute coronary syndrome. *N Engl J Med* 1992;326:242–50.
- Varnava AM, Mills PG, Davies MJ. Relationship between coronary artery remodeling and plaque vulnerability. *Circulation* 2002;105:939–43.
- Virmani R, Kolodgie FD, Burke AP, et al. Lesson from sudden coronary death: a comprehensive morphological classification scheme for atherosclerotic lesions. *Arterioscler Thromb Vasc Biol* 2000;20:1262–75.
- Hackett D, Davies G, Maseri A. Preexisting coronary stenoses in patients with first myocardial infarction are not necessarily severe. *Eur Heart J* 1988;9:1317–23.
- Ambrose JA, Tannenbaum MA, Alexopoulos D, et al. Angiographic progression of coronary artery disease and the development of myocardial infarction. *J Am Coll Cardiol* 1988;12:56–62.
- Nissen SE, Yock P. Intravascular ultrasound: novel diagnostic insights and current clinical application. *Circulation* 2001;103:604–16.
- Glagov S, Weisenberg E, Zarins CK, et al. Compensatory enlargement of human atherosclerotic coronary arteries. *N Engl J Med* 1987;316:1371–5.
- Kawasaki M, Takatsu H, Noda T, et al. In vivo quantitative tissue characterization of human coronary arterial plaques by use of integrated backscatter intravascular ultrasound and comparison with angiographic findings. *Circulation* 2002;105:2487–92.
- Kawasaki M, Sano K, Okubo M, et al. Volumetric quantitative analysis of tissue characteristics of coronary plaques after statin therapy using three dimensional integrated backscatter intravascular ultrasound. *J Am Coll Cardiol* 2005;45:1946–53.
- Sano K, Kawasaki M, Okubo M, et al. In vivo quantitative tissue characterization of angiographically normal coronary lesions and the relation with risk factors—a study using integrated backscatter intravascular ultrasound. *Circulation J* 2005;69:543–9.
- Komiyama N, Berry G, Kolz M, et al. Tissue characterization of atherosclerotic plaques by intravascular ultrasound radio frequency signal analyses. An in vitro study of human coronary arteries. *Am Heart J* 2000;140:565–74.
- Murashige A, Hiro T, Fujii T, et al. Detection of lipid-laden atherosclerotic plaque by Wavelet analysis of radiofrequency intravascular ultrasound signals. In vitro validation and preliminary in vivo application. *J Am Coll Cardiol* 2005;45:1954–60.
- Schaar AJ, de Korte CL, Mastik F, et al. Characterizing vulnerable plaque features with intravascular elastography. *Circulation* 2003;108:2636–41.
- Nair A, Kuban BD, Tuzcu EM, et al. Coronary plaque classification with intravascular ultrasound radiofrequency data analysis. *Circulation* 2002;106:2200–6.
- Lichten P, Nikutta P, Jost S, et al. Anatomical progression of coronary artery disease in humans as seen by prospective, repeated, quantitated coronary angiography. Relation to clinical events and risk factors. *Circulation* 1992;86:828–38.
- Bruschke AVG, Kramer JR, Bal ET, et al. The dynamics of progression of coronary atherosclerosis studies in 168 medically treated patients who underwent coronary arteriography three times. *Am Heart J* 1989;117:296–305.
- Uchida Y, Nakamura F, Tomaru T, et al. Prediction of acute coronary syndromes by percutaneous coronary angiography in patients with stable angina. *Am Heart J* 1995;130:195–203.
- Yamagishi M, Terashima M, Awano K, et al. Morphology of vulnerable coronary plaque: insights from follow-up of patients examined by intravascular ultrasound before an acute coronary syndrome. *J Am Coll Cardiol* 2000;35:106–11.
- Schartl M, Bocksch W, Koshyk DH, et al. Use of intravascular ultrasound to compare effects of different strategies of lipid-lowering therapy on plaque volume and composition in patients with coronary artery disease. *Circulation* 2001;104:387–92.
- Nissen SE, Tuzcu EM, Schoenhagen P, et al. Effect of intensive compared with moderate lipid-lowering therapy on progression of coronary atherosclerosis: a randomized controlled trial. *JAMA* 2004;291:1071–80.
- Glaser R, Selzer F, Faxon DF, et al. Clinical progression of incidental, asymptomatic lesions discovered during culprit vessel coronary intervention. *Circulation* 2005;111:143–9.
- Rioufol G, Finet G, Ginon I, et al. Multiple atherosclerotic plaque rupture in acute coronary syndrome: a three-vessel intravascular ultrasound study. *Circulation* 2002;106:804–8.
- Asakura M, Ueda Y, Yamaguchi O, et al. Extensive development of vulnerable plaques as a pan-coronary process in patients with myocardial infarction: an angiographic study. *J Am Coll Cardiol* 2001;37:1284–8.
- Maehara A, Mintz GS, Bui AB, et al. Morphologic and angiographic features of coronary plaque rupture detected by intravascular ultrasound. *J Am Coll Cardiol* 2002;40:904–10.
- Fujii K, Kobayashi Y, Minz GS, et al. Intravascular ultrasound assessment of ulcerated ruptured plaques. A comparison of culprit and nonculprit lesions of patients with acute coronary syndromes and lesions in patients without acute coronary syndromes. *Circulation* 2003;108:2473–8.
- Nakamura M, Nishikawa H, Mukai S, et al. Impact of coronary artery remodeling on clinical presentation of coronary disease: an intravascular ultrasound study. *J Am Coll Cardiol* 2001;37:63–9.
- von Birgelen C, Klinkhart W, Mintz GS, et al. Plaque distribution and vascular remodeling of ruptured and nonruptured coronary plaques in the same vessel: an intravascular ultrasound study in vivo. *J Am Coll Cardiol* 2001;37:1864–70.
- Davies MJ, Richardson PD, Woolf N, et al. Risk of thrombosis in human atherosclerotic plaques: role of extracellular lipid, macrophage, and smooth muscle cell content. *Br Heart J* 1993;69:377–81.
- Cheng GC, Loree HM, Kamm RD, et al. Distribution of circumferential stress in ruptured and stable atherosclerotic lesions: a structural analysis with histopathological correlation. *Circulation* 1993;87:1179–87.

**Assessment of Vulnerable Plaques Causing Acute Coronary Syndrome Using
Integrated Backscatter Intravascular Ultrasound**

Keiji Sano, Masanori Kawasaki, Yoshiyuki Ishihara, Munenori Okubo, Kunihiro
Tsuchiya, Kazuhiko Nishigaki, Xiangrong Zhou, Shinya Minatoguchi, Hiroshi
Fujita, and Hisayoshi Fujiwara

J. Am. Coll. Cardiol. published online Feb 6, 2006;

doi:10.1016/j.jacc.2005.09.061

This information is current as of February 10, 2012

Updated Information & Services	including high-resolution figures, can be found at: http://content.onlinejacc.org/cgi/content/full/j.jacc.2005.09.061v1
References	This article cites 30 articles, 22 of which you can access for free at: http://content.onlinejacc.org/cgi/content/full/j.jacc.2005.09.061v1#BIBL
Citations	This article has been cited by 15 HighWire-hosted articles: http://content.onlinejacc.org/cgi/content/full/j.jacc.2005.09.061v1#otherarticles
Rights & Permissions	Information about reproducing this article in parts (figures, tables) or in its entirety can be found online at: http://content.onlinejacc.org/misc/permissions.dtl
Reprints	Information about ordering reprints can be found online: http://content.onlinejacc.org/misc/reprints.dtl